


Cupratelike electronic and magnetic properties of layered transition-metal difluorides from first-principles calculations

Clark Miller^{✉*} and Antia Sanchez Botana*Department of Physics, Arizona State University, Tempe, Arizona, 85287, USA*

 (Received 3 January 2020; revised manuscript received 14 April 2020; accepted 15 April 2020; published 11 May 2020)

The electronic and magnetic properties of two isoelectronic layered transition-metal fluorides (AgF_2 and CuF_2) are considered in the context of high-temperature superconducting cuprates. The properties of AgF_2 are found to be cupratelike comprising a layered spin- $\frac{1}{2}$ system with strong p - d hybridization, and a large two-dimensional antiferromagnetic superexchange interaction, comparable to cuprates. Contrary to its Ag-counterpart, CuF_2 shows a small degree of p - d hybridization and a superexchange interaction one order of magnitude smaller than in cuprates. Within the Zaanen-Sawatzky-Allen model AgF_2 and CuF_2 could be classified as a charge-transfer and Mott-Hubbard insulator, respectively. As a consequence, this work further demonstrates the promise AgF_2 holds as a parent compound to a new class of Ag-based superconducting materials, whereas CuF_2 is not promising as a cuprate analog.

DOI: [10.1103/PhysRevB.101.195116](https://doi.org/10.1103/PhysRevB.101.195116)

I. INTRODUCTION

The exact mechanism that gives rise to high-temperature superconductivity in the cuprates remains a major unsolved problem in condensed-matter physics. Among different approaches to address this problem, finding cuprate-analogs has been an obvious strategy. The collection of structural, electronic, and magnetic characteristics considered to be proxies for cuprate physics include a layered structure based on two-dimensional (2D) CuO_2 planes, a parent phase with Cu^{2+} : d^9 configuration, spin- $\frac{1}{2}$ antiferromagnetic (AFM) correlations, large superexchange interactions, a large degree of p - d hybridization, and the involvement of a single band of $d_{x^2-y^2}$ character around the Fermi level [1,2].

Identification of materials likely to replicate these cuprate-like features can proceed by replacing Cu with other $3d$ or $4d$ transition-metal (TM) elements, searching for alternate ligands, or adjusting both constituent elements. One proposal has been to look at nickelates, as Ni and Cu are next to each other in the periodic table. Some of the most intensively studied nickelates include LaNiO_3 -based heterostructures [3,4] and La_2NiO_4 [5], with Ni^{3+} (d^7) and Ni^{2+} (d^8), respectively. The cupratelike Cu^{2+} : d^9 configuration, however, requires the highly unusual valence Ni^{1+} [6] as found in $R\text{NiO}_2$ ($R = \text{La}, \text{Nd}$) [7]. Intriguingly, strontium-doped NdNiO_2 has recently been observed to exhibit superconductivity at relatively high temperatures, $9 \text{ K} \leq T_c \leq 15 \text{ K}$ [8]. Another obvious strategy is to move down in the periodic table and substitute Cu by Ag. However, Ag is known to be a valence skipper that prefers to be Ag^{1+} or Ag^{3+} [9]. The instability of Ag^{2+} is due to a large electron affinity which makes this species a potent oxidizer typically capable of reclaiming an electron and returning to Ag^{1+} [10]. In this respect, it becomes beneficial

to counterbalance the large (second) ionization potential of silver with the extreme electronegativity of fluorine. Here one expects to find the fluorine $2p$ energies to lie between the second and third oxidation states of silver, mimicking the cuprate scenario for the $\text{O}(2p)$ energies relative to the Cu^{2+} states [11]. Thereby, this indicates a strong likelihood for fluoroargentates to exhibit cupratelike physics.

AgF_2 is indeed similar to cuprates in that it is a layered system where Ag is found in a $2+$ state (isoelectronic to Cu^{2+}). AgF_2 has a Cu counterpart CuF_2 in which Cu is also in a $2+$: d^9 configuration. Both materials are based on the same structural motifs of transition-metal ions bonded with four fluorines in a near-square-planar configuration [12]. These square units interlink via a single F to form each layer. Importantly, it is also found that the magnetic structures of silver and copper difluoride are quite similar [13]. The characteristic buckled planes of both materials have AFM checker-board configurations in which magnetic moments anti-align parallel to these planes resulting in a 2D magnetization [13,14]. Measurements show ordered magnetic moments of similar magnitude, $\mu_{\text{AgF}_2} = 0.70 \mu_B$ [13] and $\mu_{\text{CuF}_2} = 0.73 \mu_B$ [14], but different Curie-Weiss temperatures, $\Theta_{\text{AgF}_2} = -715 \text{ K}$ [13] and $\Theta_{\text{CuF}_2} = -200 \text{ K}$ [15].

Recently, a silver route to superconductivity has been proposed based on studies of AgF_2 [16,17]. This characterization is based on estimates of a large superexchange interaction (-70 meV) which results from analysis of a two-magnon state identified in Raman-scattering spectra [17]. Given this renewed interest in exploring superconductivity within the family of layered TM fluorides it is worthwhile to reconsider AgF_2 and the related CuF_2 with respect to their cuprate-like properties. Here, we analyze the electronic structure and magnetic properties of AgF_2 and CuF_2 by using first principles calculations. We find AgF_2 is similar to cuprates in comprising a layered spin- $\frac{1}{2}$ system, demonstrating large p - d hybridization, with large 2D AFM superexchange (SE)

*camill38@asu.edu

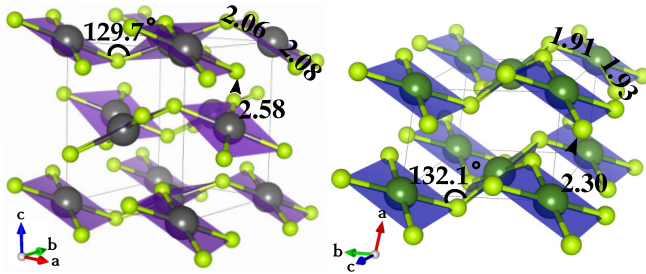


FIG. 1. (left) AgF_2 in the orthorhombic structure of $Pbca$ space group symmetry. (right) CuF_2 in the monoclinic structure with $P2_1/c$ space group symmetry. Both diagrams indicate octahedral bond lengths (\AA) and planar buckling angle (degrees). The square-planar coordination of each TM-ion [Ag^{2+} (dark gray), Cu^{2+} (green)] by F^- ions (yellow) is shown.

interactions (of half the strength found in cuprates). In contrast, its Cu counterpart CuF_2 exhibits a pronounced ionic character with very little p - d hybridization and, although structurally similar to AgF_2 , the buckled layers demonstrate SE couplings that are one-tenth the strength found in cuprates.

II. STRUCTURAL PROPERTIES

Experimentally it has been shown that AgF_2 crystallizes in an orthorhombic structure with $Pbca$ space group symmetry, as seen in Fig. 1 (left). The structural units are [AgF_4] plaquettes characterized by the nearly-square-planar coordination by F^- ions of each Ag^{2+} ion, with in-plane bond lengths of 2.06 and 2.08 \AA at angles that deviate by $\approx \pm 3^\circ$ from 90° . These squares are the result of the cooperative Jahn-Teller axial distortion of [AgF_6] octahedra with elongated out-of-plane bonds of 2.58 \AA . Each of these [AgF_4] squares is corner-linked by a common F^- ion at a 129.7° angle. This proceeds in a chessboard-like manner and forms puckered layers of [AgF_4] parallel to the (001) plane. These corrugated sheets then stack in a staggered manner along the crystallographic c axis to complete the structure.

A similar structure has been reported for copper difluoride, shown in Fig. 1 (right). The crystal structure is monoclinic with $P2_1/c$ space group symmetry where square-planar coordination by F^- ions of each Cu^{2+} ion forms the characteristic [CuF_4] square units. Here, these feature in-plane bond lengths of 1.91 and 1.93 \AA at angles which deviate by $\approx \pm 0.4^\circ$ from 90° . These [CuF_4] squares are corner-linked by a shared F^- ion at a 132.1° angle forming the buckled planes. Similarly to its Ag counterpart, the cooperative Jahn-Teller axial distortion of [CuF_6] octahedra gives rise to an elongated out-of-plane bond length of 2.30 \AA . In contrast to AgF_2 , here the puckered layers of [CuF_4] squares form parallel to the (100) plane and stack along the a axis.

A monoclinic unit cell can also be used to characterize silver difluoride with $P2_1/c$ symmetry. This gives an isostructural description of Cu and Ag isoelectronic counterparts. Notice that this description modifies the geometry of the characteristic [AgF_4] squares by increasing the in-plane bond lengths to 2.11 and 2.13 \AA where the associated in-plane angles are at $90^\circ \pm 0.7^\circ$. Similarly, the planar buckling angle is increased here to 135.8° , while the out-of-plane bond length

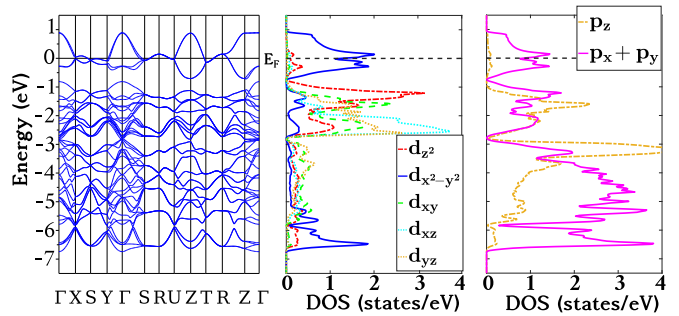


FIG. 2. Band structure and F- p , Ag- d orbital-resolved DOS resulting from the nonmagnetic GGA calculation of AgF_2 within the experimentally reported $Pbca$ structure. Note the $d_{x^2-y^2}$ character of the band crossing the Fermi level as matching expectations from an ionic description.

is 2.62 \AA . The impact these deviations have on the resulting electronic structure of AgF_2 is considered below.

III. COMPUTATIONAL DETAILS

This work presents density-functional theory (DFT) calculations performed with the WIEN2K [18] simulation package. This is an all electron, full-potential method implementing a basis-set of (linearized) augmented plane waves and local orbitals [(L)APW+LO]. For unpolarized calculations the exchange-correlation (XC) functional chosen is the generalized gradient approximation (GGA) of Perdew, Burke, and Ernzerhof [19]. To better account for the strongly correlated nature of the d -electrons, spin-polarized calculations were performed by using three different methods for approximating the XC interaction: (i) HSE06 [20] from the class of hybrid density functionals, (ii) GGA + U [21] in which an on-site Coulomb repulsion is included, and (iii) modified Beck-Johnson [22] from the class of multiplicative-exchange (orbital-independent) potentials.

The results of computations using the WIEN2K approximation to the hybrid HSE06 functional [23] will be referred to as HSE06. The findings obtained using the (Tran-Blaha) modified Becke-Johnson semilocal XC potential will be abbreviated as TB-mBJ. For GGA + U , two values were used for the on-site Coulomb repulsion energy U_d , (i) $U_d = 5.0 \text{ eV}$ [24,25], and (ii) $U_d = 9.4 \text{ eV}$ [26]. Both of these on-site energies were defined in conjunction with an (on-site) exchange term J , which remained set at $J = 1.0 \text{ eV}$ [21].

Computations performed within monoclinic structures were converged on a $16 \times 12 \times 12$ \mathbf{k} mesh with basis-set cut-off parameter $R_{\mathbf{k},\text{max}} = 7.75$, while the orthorhombic structure converged calculations on a $16 \times 16 \times 16$ \mathbf{k} mesh with $R_{\mathbf{k},\text{max}} = 7.55$. The muffin-tin radius (a.u.) for F was 1.71 for all material settings, while being 2.03 for Ag and 1.89 for Cu.

IV. RESULTS

In a simple ionic picture, the silver and copper atoms are predicted to be in a $2+$ oxidation state (d^9 configuration). For a d^9 ion in a square-planar environment the expectation is to have a single hole in the $d_{x^2-y^2}$ orbital. Figure 2 shows

TABLE I. Magnetic moments (in μ_B), AFM insulating band gaps (in eV), and magnetic coupling constants (in meV) obtained using various XC potentials for each material. At top the dash-marks indicate the instability of the FM spin-configuration for the GGA calculation of AgF_2 in the $Pbca$ setting. This calculation converged to the AFM configuration and the corresponding values.

DFT method	$\pm\mu_{\text{AFM}}$	μ_{FM}	$E_{\text{gap}}^{\text{AFM}}$	$ J_{2D} $
$\text{AgF}_2 - Pbca$				
GGA	0.36		0.19	
GGA + 5 eV	0.61	0.66	1.78	51
GGA + 9.4 eV	0.73	0.75	3.55	29
HSE06	0.64	0.69	2.52	63
TB-mBJ	0.66	N/A	1.86	N/A
$\text{CuF}_2 - P2_1/c$				
GGA	0.63	0.75	0.30	24
GGA + 5 eV	0.80	0.82	2.29	17
GGA + 9.4 eV	0.88	0.88	4.87	9
HSE06	0.83	0.85	4.21	1
TB-mBJ	0.89	N/A	3.06	N/A

the nonmagnetic GGA band structure of AgF_2 ($Pbca$ space group) which is metallic due to the odd number of electrons per cell. Here, a single band per Ag-atom of $d_{x^2-y^2}$ character can be seen crossing the Fermi level, demonstrating that the unpolarized GGA calculation yields an ionic-level description. The analogous calculation of CuF_2 (not shown) was found to be metallic and likewise in keeping with the ionic model.

However, the magnetic nature of a d^9 ion provides an expectation to find these materials in a magnetically ordered ground state. To ascertain the nature and impact of this ordering, spin-polarized GGA calculations were performed in both ferromagnetic (FM) and antiferromagnetic configurations. From these calculations it was found that both AgF_2 ($Pbca$ and $P2_1/c$ settings) and CuF_2 have checker-board AFM ground-state configurations. This magnetic ordering was found to produce insulating ground states at the GGA level with band gaps in CuF_2 of 0.30 eV and AgF_2 of 0.19 eV (as described with $Pbca$ space group symmetry). In the $P2_1/c$ structure, GGA gives a metallic ground state for AgF_2 .

To better account for the strongly correlated nature of the d electrons, calculations were performed by using HSE06, GGA + U , and TB-mBJ. Table I shows the resulting magnetic moments, values of the band gap, and magnetic coupling constant for each case. Notice TB-mBJ is only an XC potential, meaning that it cannot be obtained as the derivative of an energy functional [27,28], i.e., TB-mBJ calculations are not self-consistent with respect to the total energy. As a result, magnetic couplings cannot be obtained from spin-polarized TB-mBJ calculations [29].

Figure 3 (top) presents the AFM TB-mBJ calculated electronic structure of AgF_2 in terms of the F- p , Ag- d orbital-resolved density of states (DOS) resulting from the experimental $Pbca$ structure [12]. This calculation gives rise to an insulating gap of 1.86 eV, and an atomic magnetic moment of $\mu_{\text{Ag}} = \pm 0.66 \mu_B$ per Ag atom. The band gap separates states that are predominantly $d_{x^2-y^2}$ at the conduction-band minimum (CBM) from states that are relatively equal mixtures

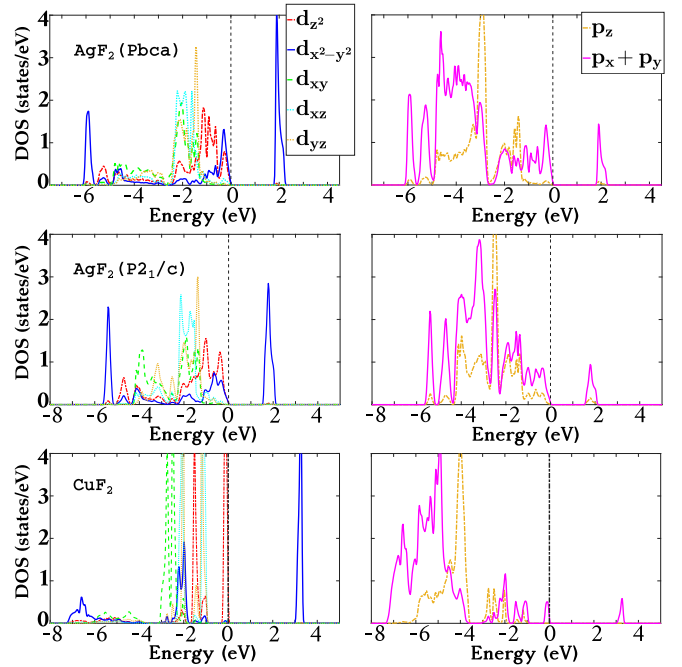


FIG. 3. Comparison of AFM TB-mBJ electronic structures in terms of the F- p , TM- d orbital-resolved DOS. (top and middle) Calculations on AgF_2 as depicted in the experimentally verified $Pbca$ structure (top) and in the monoclinic structure (middle) of $P2_1/c$ space group symmetry. (bottom) Results for CuF_2 described in the experimentally verified monoclinic ($P2_1/c$) structure.

of d_{z^2} , $d_{x^2-y^2}$, and $p_x + p_y$ at the valence-band maximum (VBM). The valence bandwidth is ≈ 6 eV and spans the F- p and Ag- d spectral components, demonstrating a high-degree of p - d hybridization. These DOS indicate a strongly covalent bond exists between Ag and F, matching similar conclusions from experimental x-ray photoelectron spectra (XPS) [30]. Within the Zaanen-Sawatzky-Allen (ZSA) model [31] the nature of this band gap indicates that AgF_2 is a charge-transfer insulator. We note that in cuprates the high degree of p - d hybridization has been directly correlated with T_c in dynamical mean-field theory studies [2,32].

Figure 4 compares this AFM TB-mBJ (top) electronic structure of AgF_2 with the AFM electronic structure resulting from the far more computationally costly HSE06 method (bottom). Here, one finds a high degree of agreement in the electronic structure and magnetic moments obtained within the TB-mBJ and hybrid functionals. Only a change in the value of the band gap is found, 1.86 eV (TB-mBJ) vs 2.52 eV (HSE06). Our results agree with HSE06 results reported in Ref. [17]. These findings provide further demonstration of the well-documented accuracy of the TB-mBJ potential at considerably lower computational cost than hybrids [22,33]. Notably, TB-mBJ has been applied to $\text{YBa}_2\text{Cu}_3\text{O}_6$ and produced good agreement with experimental values of the band gap, magnetic moment, and electric-field gradient [33].

Figure 3 (bottom) displays the AFM TB-mBJ calculated electronic structure of CuF_2 in terms of the F- p , Cu- d orbital-resolved DOS. This calculation shows an insulating band gap of 3.06 eV, while predicting a magnetic moment for Cu of $\mu_{\text{Cu}} = \pm 0.89 \mu_B$. Here the CBM is mainly composed of

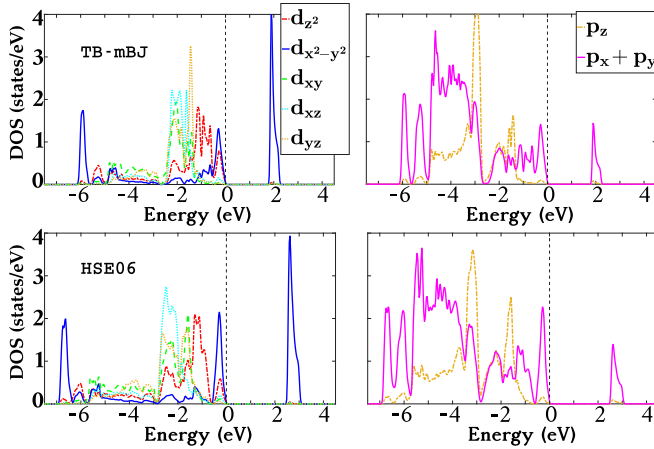


FIG. 4. Comparison of the electronic structure of AgF_2 in terms of the F- p , Ag- d orbital-resolved DOS in AFM spin-polarized calculations within the experimental $Pbca$ structure. (top) Computations performed using TB-mBJ. (bottom) Results using HSE06.

$d_{x^2-y^2}$ states while the VBM states are predominantly d_{z^2} and given by exceedingly narrow, peaked bands indicating very little ligand p -like contributions. Immediately “below” these VBM d_{z^2} states there is an intra- d band gap where the $d_{x^2-y^2}$ antibonding states have been shifted beneath the same-spin d_{z^2} states. In addition, there is a clear separation in energy between states of p - and d -like character thereby illustrating a much lower degree of p - d hybridization as compared with AgF_2 and cuprates. Accordingly, these orbital-resolved distributions largely describe CuF_2 as an ionic compound. The nature of the band gap depicts copper difluoride as a Mott-Hubbard-type insulator, as per the ZSA model [31], in contrast with AgF_2 .

Figure 3 (middle) presents the AFM TB-mBJ calculated electronic structure of AgF_2 in terms of the F- p , Ag- d orbital-resolved DOS resulting from the monoclinic space group $P2_1/c$. The insulating gap was found to be 1.60 eV, with magnetic moments for the Ag atoms $\mu_{\text{Ag}} = \pm 0.66 \mu_B$. Comparing the AgF_2 description in both settings shows that the F- p and Ag- d orbital components retain the general aspects of their relative spectral-distributions. Transference to the $P2_1/c$ space group only slightly alters some of the characteristics of the valence band. In particular, the total valence bandwidth is seen to have compressed by ≈ 0.5 eV. This can be attributed to the slightly decreased overlap of the $p(\text{F})$ and $d(\text{Ag})$ orbitals stemming from the increased bond lengths in the monoclinic cell [34]. However, these effects are mitigated by the increased perpendicular orientation of the in-plane F–Ag–F bond angles and the simplified stacking formation of the monoclinic setting. All in all, the main electronic structure features of AgF_2 are the same in the $P2_1/c$ and $Pbca$ settings. This indicates that the differences in electronic structure between CuF_2 and AgF_2 cannot be attributed to differences in space group.

The AFM TB-mBJ results for AgF_2 and CuF_2 can then be utilized as a guide to map trends in the results of Table I in terms of magnetic moments and band-gap values. Regarding AgF_2 , GGA + U ($U_d = 5$ eV) and HSE06 are seen to provide much better agreement with TB-mBJ band gaps and magnetic moments than GGA + U ($U_d = 9.4$ eV). Similar analysis of

CuF_2 from Table I suggests that an on-site Coulomb repulsion of 9.4 eV gives similar results for the magnetic moments to TB-mBJ but at the cost of overstating the band gap. GGA + U ($U_d = 5$ eV) underestimates the insulating gap and gives rise to magnetic moments smaller than TB-mBJ. HSE06 both overestimates the band gap and underestimates the magnetic moments compared with TB-mBJ.

The magnetic coupling constants were obtained for a given XC functional by fitting the difference in energies associated with different magnetic configurations to a Heisenberg Hamiltonian,

$$H = - \sum_{\langle i,j \rangle} J_{ij} S_i S_j. \quad (1)$$

Here J_{ij} is the magnetic coupling constant, while S_i and S_j represent the spin of the respective TM site. The choice of the sign in Eq. (1) yields AFM interactions for $J_{ij} < 0$. We limited ourselves to nearest-neighbor interactions which are contained within the buckled planes for these materials. This is noted as J_{2D} herein. For each material the various $|J_{2D}|$ seen in Table I are then reconciled with the consistent description outlined above.

In AgF_2 , GGA + U ($U_d = 5$ eV) and HSE06 give magnetic couplings of comparable strength, $J_{2D} = -51$ meV and $J_{2D} = -63$ meV, respectively. These values are similar to the estimation resulting from the experimental Curie-Weiss temperature, which gives $J_{2D} \approx -62$ meV by assuming the dominance of nearest-neighbor interactions. They also agree with the value obtained from a hybrid-functional computation (-56 meV) [35]. The recent two-magnon Raman-scattering estimate [17] is slightly larger (-70 meV). We can compare these estimates for AgF_2 with the SE couplings found in cuprates, e.g., La_2CuO_4 (-135 meV) [36,37] obtaining $J_{2D}^{\text{AgF}_2} \approx \frac{1}{2} J_{2D}^{\text{La}_2\text{CuO}_4}$.

Regarding CuF_2 , within the GGA + U methods we obtain $J_{2D} = -9$ meV ($U_d = 9.4$ eV), and $J_{2D} = -17$ meV ($U_d = 5$ eV). This range is found to capture a difference dedicated configuration-interaction calculation (-11.4 meV) [38]. It also agrees with the value estimated from the Curie-Weiss temperature $J_{2D} \approx -9$ meV from nearest-neighbor interactions. This indicates that CuF_2 indeed hosts a SE interaction that is smaller than that of its Ag counterpart, $J_{2D}^{\text{CuF}_2} \approx \frac{1}{5} J_{2D}^{\text{AgF}_2}$, and much smaller than typical of cuprates, $J_{2D}^{\text{CuF}_2} \approx \frac{1}{10} J_{2D}^{\text{La}_2\text{CuO}_4}$.

V. CONCLUSION

Our electronic structure calculations demonstrate that AgF_2 is a highly covalent system with large p - d hybridization, in agreement with experiments [30]. Within the ZSA model [31], AgF_2 is classified as a charge-transfer insulator. We obtain a large superexchange interaction, $J_{2D} \approx -60$ meV of approximately half the strength of cuprate parent compounds. Contrary to this description, we find that CuF_2 is a largely ionic system that can be classified within the ZSA model [31] as a Mott-Hubbard-type insulator. We obtain values of the magnetic couplings of $J_{2D} \approx -12$ meV, much smaller than its Ag counterpart ($J_{2D}^{\text{CuF}_2} \approx \frac{1}{5} J_{2D}^{\text{AgF}_2}$) and an order-of-magnitude smaller than that found in the cuprates.

Therefore, these results demonstrate that AgF_2 exhibits cupratelike properties to a large degree; with strong p - d hybridization, hosting large 2D AFM magnetic interactions of half-the strength of cuprate parent compounds. Regarding CuF_2 we find a lesser degree of cupratelike characteristics; although similarly comprising a 2D layered system, there is a pronounced ionic character with very little p - d hybridization, while hosting an intraplanar SE coupling of one-tenth the strength of the cuprates. Taking these properties as meaningful markers of cupratelike behavior, we find that AgF_2 is a promising candidate for experimental consideration as a

parent compound to new high- T_c materials, whereas its Cu counterpart is not promising.

ACKNOWLEDGMENTS

We acknowledge Research Computing at Arizona State University for providing HPC and storage resources necessary for the research results reported within this paper (see <https://cores.research.asu.edu>). CM thanks Arizona State University for startup funds. ASB acknowledges NSF-DMR grant 1904716.

-
- [1] M. R. Norman, *Rep. Prog. Phys.* **79**, 074502 (2016).
- [2] C. Weber, C. Yee, K. Haule, and G. Kotliar, *Europhys. Lett.* **100**, 37001 (2012).
- [3] J. Chaloupka and G. Khaliullin, *Phys. Rev. Lett.* **100**, 016404 (2008).
- [4] P. Hansmann, X. Yang, A. Toschi, G. Khaliullin, O. K. Andersen, and K. Held, *Phys. Rev. Lett.* **103**, 016401 (2009).
- [5] V. I. Anisimov, D. Bukhalov, and T. M. Rice, *Phys. Rev. B* **59**, 7901 (1999).
- [6] K.-W. Lee and W. E. Pickett, *Phys. Rev. B* **70**, 165109 (2004).
- [7] G. A. Sawatzky, *Nature (London)* **572**, 592 (2019).
- [8] D. Li, K. Lee, B. Y. Wang, M. Osada, S. Crossley, H. R. Lee, Y. Cui, Y. Hikita, and H. Y. Hwang, *Nature (London)* **572**, 624 (2019).
- [9] W. Grochala, *Nat. Mater.* **5**, 513 (2006).
- [10] W. Grochala and Z. Mazej, *Philos. Trans. R. Soc., A* **373**, 20140179 (2015).
- [11] W. Grochala and R. Hoffmann, *Angew. Chem. Int. Ed.* **40**, 2742 (2001).
- [12] P. Fischer, D. Schwarzenbach, and H. M. Rietveld, *J. Phys. Chem. Solids* **32**, 543 (1971).
- [13] P. Fischer, G. Roullet, and D. Schwarzenbach, *J. Phys. Chem. Solids* **32**, 1641 (1971).
- [14] P. Fischer, W. Hälg, D. Schwarzenbach, and H. Gamsjäger, *J. Phys. Chem. Solids* **35**, 1683 (1974).
- [15] R. J. Joenk and R. M. Bozorth, *J. Appl. Phys.* **36**, 1167 (1965).
- [16] D. Kurzydłowski, M. Derzsi, P. Barone, A. Grzelak, V. Struzhkin, J. Lorenzana, and W. Grochala, *Chem. Commun.* **54**, 10252 (2018).
- [17] J. Gawraczyński, D. Kurzydłowski, R. A. Ewings, S. Bandaru, W. Gadamski, Z. Mazej, G. Ruani, I. Bergenti, T. Jaroń *et al.*, *Proc. Natl. Acad. Sci. U. S. A.* **116**, 1495 (2019).
- [18] P. Blaha, K. Schwarz, G. K. H. Madsen, D. Kvasnicka, J. Luitz, R. Laskowski, F. Tran, and L. D. Marks, *WIEN2k, An Augmented Plane Wave + Local Orbitals Program for Calculating Crystal Properties* (Karlheinz Schwarz, Techn. Universität Wien, 2018).
- [19] J. P. Perdew, K. Burke, and M. Ernzerhof, *Phys. Rev. Lett.* **77**, 3865 (1996); **78**, 1396 (1997).
- [20] A. V. Krukau, O. A. Vydrov, A. F. Izmaylov, and G. E. Scuseria, *J. Chem. Phys.* **125**, 224106 (2006).
- [21] V. I. Anisimov, J. Zaanen, and O. K. Andersen, *Phys. Rev. B* **44**, 943 (1991).
- [22] F. Tran and P. Blaha, *Phys. Rev. Lett.* **102**, 226401 (2009).
- [23] F. Tran and P. Blaha, *Phys. Rev. B* **83**, 235118 (2011).
- [24] X. Zhang, G. Zhang, T. Jia, Y. Guo, Z. Zeng, and H. Lin, *Phys. Lett. A* **375**, 2456 (2011).
- [25] D. Kasinathan, K. Koepf, U. Nitzsche, and H. Rosner, *Phys. Rev. Lett.* **99**, 247210 (2007).
- [26] L. H. Tjeng, M. B. J. Meinders, J. van Elp, J. Ghijsen, G. A. Sawatzky, and R. L. Johnson, *Phys. Rev. B* **41**, 3190 (1990).
- [27] A. Karolewski, R. Armiento, and S. Kümmel, *J. Chem. Theory Comput.* **5**, 712 (2009).
- [28] A. P. Gaiduk and V. N. Staroverov, *J. Chem. Phys.* **131**, 044107 (2009).
- [29] F. Illas, I. de P. R. Moreira, C. de Graaf, and V. Barone, *Theor. Chem. Acta* **104**, 265 (2000).
- [30] W. Grochala, R. G. Egdell, P. P. Edwards, Z. Mazej, and B. Žemva, *ChemPhysChem* **4**, 997 (2003).
- [31] J. Zaanen, G. A. Sawatzky, and J. W. Allen, *Phys. Rev. Lett.* **55**, 418 (1985).
- [32] P. Hansmann, N. Parragh, A. Toschi, G. Sangiovanni, and K. Held, *New J. Phys.* **16**, 033009 (2014).
- [33] D. Koller, F. Tran, and P. Blaha, *Phys. Rev. B* **83**, 195134 (2011).
- [34] D. I. Khomskii, *Transition Metal Compounds* (Cambridge University Press, Cambridge (England), 2014).
- [35] D. Kurzydłowski and W. Grochala, *Angew. Chem., Int. Ed.* **56**, 10114 (2017).
- [36] M. A. Kastner, R. J. Birgeneau, G. Shirane, and Y. Endoh, *Rev. Mod. Phys.* **70**, 897 (1998).
- [37] S. M. Hayden, G. Aeppli, R. Osborn, A. D. Taylor, T. G. Perring, S.-W. Cheong, and Z. Fisk, *Phys. Rev. Lett.* **67**, 3622 (1991).
- [38] P. Reinhardt, I. de P. R. Moreira, C. de Graaf, R. Dovesi, and F. Illas, *Chem. Phys. Lett.* **319**, 625 (2000).